Chapter 3

Theoretical Model Codes

This chapter contains a brief overview of TALYS, EMPIRE, and ALICE statistical model codes which are extensively utilized for the simulation of experimentally measured charged particle and neutron induced reaction cross section results. The different level density models of these codes have been utilized for the reaction cross section predictions. A brief idea of optical models (OMP), nuclear level density models (NLDs) and gamma ray strength functions (γ-SF) is also provided in this chapter. The TALYS code is utilized for the regeneration of nuclear data of the neutron and proton activation analysis for the present study. The detail of nuclear level density models of ALICE-2014 is also given in this chapter. ALICE-2014 code has been also utilized for the cross section estimation of proton induced reactions in this work.

3.1 Introduction

Nuclear data is crucial in many fields of nuclear Physics. The importance of nuclear data was discussed for the application of nuclear astrophysics and reactors in the previous chapter. The study of different projectile (n, p, γ, α, and heavy ions) induced reactions provides a better understanding of various processes taking place while projectile incident on the target nucleus. To achieve a complete understanding of different nuclear processes for a wide range of target nuclei and projectiles, not only experimental but theoretical measurements are required. In general, three reaction mechanisms are there according to the energy range of the incident particles which were included in the different reaction models such as Compound nucleus, pre-compound, and direct reaction mechanism. The different reaction mechanism is presented in Fig. 3.1. There are several theoretical models have been designed by different authors for the theoretical calculations. These various models are ensembled in the form of computer programming into the nuclear codes that can predict data.

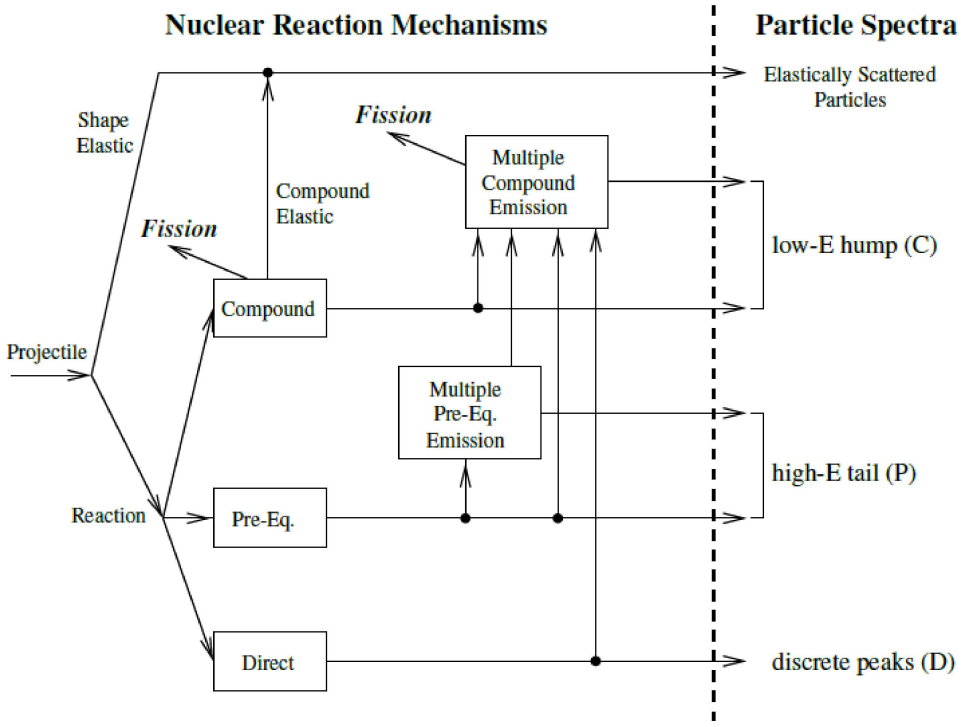

Figure 3.1: A flowchart different reaction mechanism [1].

Two types of codes are available: (1) Statistical Nuclear model codes, and (2) Nuclear transport codes. The nuclear model codes predict the data such as angular distribution of outgoing particles, different types of cross sections, gamma productions etc. Nuclear transport codes use these data to predict particle transportation in a different matter.

Nuclear model codes namely TALYS, EMPIRE, ALICE and the MCNP-nuclear transport code have been utilized for the present thesis work. The different reaction models used for the calculation are briefly discussed below.

3.2 TALYS code

TALYS provides a detailed and precise simulation of nuclear reactions of neutral particles - neutrons and photons (γ), charged particles like a proton (p), deuteron (^{2}H), triton (^{3}H), ^{3}He- and α-particles, up to 200 MeV of energy. The code accepts the target nucleus from an atomic mass of 12 and heavier. It is a user friendly and flexible code with an optimal combination and justified nuclear models. Nuclear Physics and nuclear data tools, these two main motivations are provided by TALYS. The nuclear physics tool is useful for nuclear reaction analysis purposes and the other tool provides the data at given energy for all open channels beyond the resonance region. TALYS also provides information related to angular distribution, spectra, and reaction cross sections. TALYS has been extensively used to generate nuclear data for the advancement of traditional and innovative GEN-IV nuclear power reactors, medical isotope production, homeland security, fusion reactors, transmutation of radioactive waste, oil-well logging, radiotherapy, accelerator applications, geophysics and astrophysics [1].

Various nuclear models of TALYS are classified into direct, pre-compound, compound, optical, and fission models. The parameters required for input are extracted from the RIPL input library of IAEA [2] for nuclear data prediction. The calculations of the optical model have been performed utilizing the ECIS-06 code of Raynal [3]. The global and local parameters of Koning and Delaroche are considered the de-

fault optical model potentials (OMP) [4]. The optical model calculations can also be performed using semi microscopic nucleon-nucleus spherical OMP of Jeukenne-Lejeune-Mahaux (JLM) OMP calculations [5]. The JLM OMP calculations can be performed using the MOM code of Eric Bauge [2]. The exciton model utilized for the pre-equilibrium reaction calculation was suggested by Kalbach [6] , and the Hauser Feshbach model is adopted for compound reaction mechanisms [7]. A flowchart given below shows the nuclear models of TALYS.

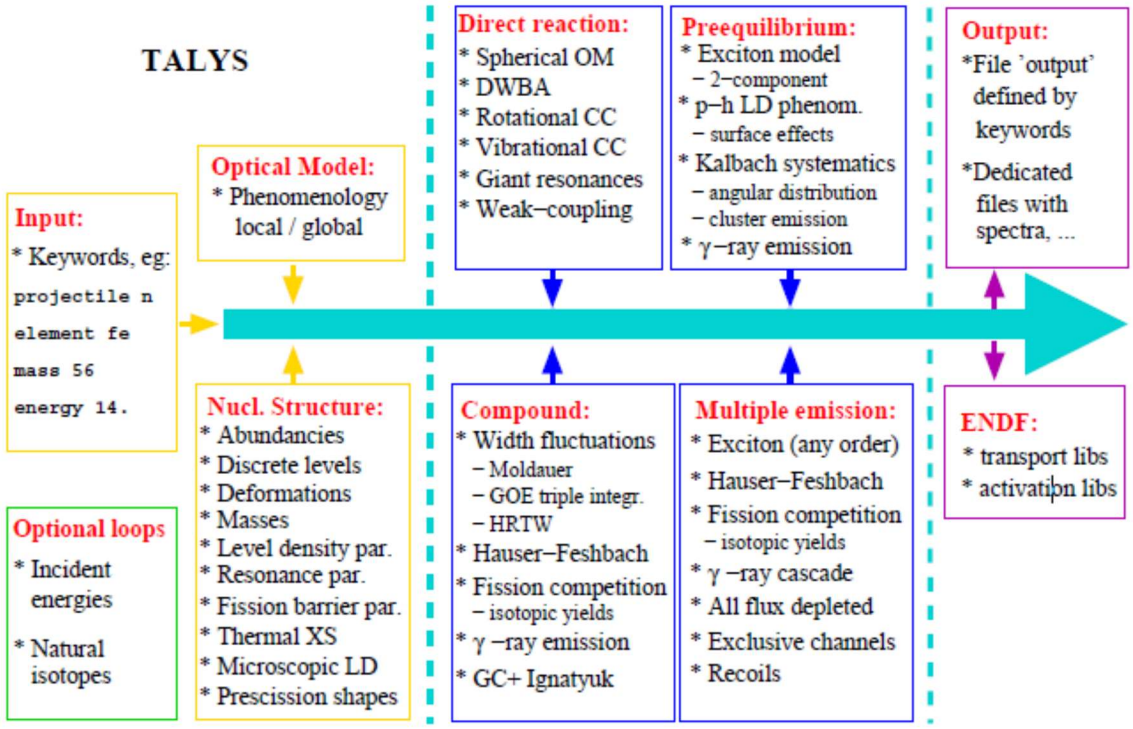

Figure 3.2: A flowchart of the nuclear models of TALYS.

3.2.1 Optical Model

Nuclear reactions can occur by the complex interplay between the target nucleus and projectile. The interaction may result in elastic scattering or cause various nuclear

reactions. If the projectile is defined as a wave then it will be absorbed or scattered classically. This phenomenon is similar to the concept of optics in which the light wave is absorbed or scattered via the complex refractive index (n) of a medium. The optical potential consists of the real part as well as the imaginary part. In the nuclear case, the imaginary part describes the inelastic scattering just the way the absorption of light in optics [8].

The complex mean-field approach is used to represent this type of interaction. The potential separates reaction flux into two categories: (i) inelastic and (ii) shape elastic scattering channels. The cross section calculation of the elastic scattering is most likely to be performed utilizing the Schrodinger equation in optical potentials. The solution provides different information namely the prediction of basic observables, angular distributions, shape elastic, reaction and total cross sections, and elastic polarization. Modification in optical parameter produces potential scattering radius R', and s- & p-wave strength functions (SF) for lower energies. The corresponding total cross sections (for neutrons) are known as the SPRT method [9]. The optical model can predict the quantities for which no measurements exist and also provide information on the not directly observable quantities.

Overall, the main motivation of the OMP is to explain the rapid, quantum mechanical preequilibrium, and direct reactions in a nuclear collision. The model can also produce the transmission coefficients that are necessary to analyze the compound nucleus studies within the statistical theory of Hauser-Feshbach.

3.2.2 Nuclear Level Density (NLD) Models

The NLD is a basic feature of atomic nuclei and can be defined as the number of nuclear levels per unit energy for definite parity (Π) and spin (J) near excitation energy. It is an essential physical quantity for the statistical calculation, reaction rate calculation of nuclear astrophysics, compound nucleus decay etc. The study of NLDs is also essential to predict the excited levels' distribution in the nucleus for nuclear physics. It is a challenging task to understand this complicated quantum mechanical system. NLDs can be used to get the discrete level information of excitation energies.

TALYS employed several level density models from phenomenological approaches to tabulated level densities obtained using the microscopic approaches.

The first three NLD options are based on phenomenological approach and others are based on the microscopic approach, are mentioned below with its keyword for input description of code.

☞ Constant Temperature + Fermi gas model (CTM) (**ldmodel 1**) [10]

- The CTM was introduced by Gilbert and Cameron by considering the available dataset and systematics, the two-level density (LD) curves are combined at a certain point in the direction of a tangent.
- The excitation energy is categorized into two parts. From 0 MeV to matching energy E_M of energy range, constant temperature law applies using the equation of level density: $\rho = N(E)/T = e^{(E-E_0)/T}$.
- The energy above matching energy E_M, the Fermi Gas Model (FGM) is applicable using NLD formula $\rho = \exp(2\sqrt{(aU)})$.

☞ **ldmodel 2**: Back-shifted Fermi gas (BFG) model [11]

- W. Dilg has developed the BFG model using a two-free parameter approach.
- The pairing energy term is considered an adjustable parameter. There are two adjustable parameters of this model: (i) the fictive ground state (GS) position δ, and (ii) the level density (LD) parameter (a)
- This model works well with the whole energy range up to 0 MeV.

☞ **ldmodel 3**: Generalised Superfluid Model (GSM) [12, 13]

- The ignored concepts like shell effects, collectivity, and pairing correlations in the CTM and FGM models were incorporated in this model.
- The concept of Bardeen-Cooper-Schrieffer (BCS) was used which includes pairing correlation into consideration.

- A. V. Ignatyuk has developed the phenomenological version of the model. At low energies, the phase transition from a superfluid behaviour was taken into consideration where level densities are strongly influenced by pairing correlations.
- The higher energy region is defined by the FGM model.
- Thus, the GSM is analogous to the CTM up to a certain energy range where low energy and a high energy range can be distinguished from each other.

☞ **ldmodel 4**: LDs from Goriely's tables [14]

- The work is motivated by considering the fact, it is not possible to study r process nucleosynthesis in the laboratory frame because it relies on the binding energy (BE) of the heavy nuclei closer to the neutron (n)-drip line. Thus, extrapolation is required for these quantities near the line of stability and out toward the n-drip line.
- The non-relativistic Hartree-Fock (HF) method along with Skyrme force was used by S. Goriely for NLD calculations.
- The level densities were tabulated for the angular momentum up to I =30 and excitation energy up to E_x = 150 MeV.

☞ **ldmodel 5**: LDs from Hilaire's combinatorial tables [15, 16]

- The combinatorial tables using a microscopic approach was developed by Hilaire and Goriely to calculate NLDs.
- Single particle level scheme of HFB is used to create the irrational particle-hole (ph) state densities defined by $\rho_{ph}(U, M, \pi)$. Here, U is the energy of excitation, M is the projection of spin on the nuclide's intrinsic symmetry axis, and π is the parity.
- After determining the irrational ph state densities, the collective effects are taken into consideration for total level density calculations.
- The tabular form contains NLDs data of more than 8500 nuclei for angular momentum up to J = 49, and excitation energy up to 200 MeV.

☞ **ldmodel 6**: TDHFB from Hilaire's combinatorial tables [16]

- The reduction of the utilization of the phenomenological approach to determine the microscopic NLDs was the prime motivation behind this work.
- The Gogny force of D1M is used rather than the Skyrme force to reduce the use of the phenomenological approach and to get the knowledge of nuclear structure from NLDs.
- The usage of Gogny force exhibited its potential to predict fairly well quadrupole collective levels, as well as vibrational and rotational levels, for lower energies.
- The model has used temperature-dependent Hartree-Fock-Bogoliubov calculations that deliver the information to deal with the structural property modification with rising excitation energies within a denser solid structure than before.

All the NLD models mentioned above, have been used in this thesis work for the theoretical predictions of data.

3.2.2.1 The level density & spin cut-off parameter

TALYS provides the facility to alter the level density parameter (LDP) to refine the fitting of the experimental data. By considering that the shell effects are present at lower energies and disappear at higher energies, the energy-dependent LDP can be defined as,

$$b = \tilde{b}\left[1 + \delta\epsilon_0\left(\frac{1 - e^{(-\gamma U)}}{U}\right)\right] \tag{3.1}$$

where,
$\tilde{b}$ = asymptotic LDP obtained when shell effects do not exist;
γ = damping parameter determines how level density (b) differs from asymptotic level density $\tilde{b}$ at low energies;
$\delta\epsilon_0$ = shell correction energy determines dependence of level density parameter (b)

on excitation energy E_x ;
U = E_x - Δ = effective excitation energy;
E_x = true excitation energy ; and
Δ = pairing energy for some models that simulate odd-even effects in the nuclide.

The formula of asymptotic value $\tilde{b}$ and systematics of damping parameter is defined as,

$$\text{asymptotic value} \quad \tilde{b} = \alpha A + \beta A^{\frac{2}{3}} \tag{3.2}$$

$$\text{damping parameter} \quad \gamma = \frac{\gamma_1}{A^{\frac{2}{3}}} + \gamma_2 \tag{3.3}$$

where, the terms used in the above equations, α, β, $\gamma_{1,2}$ are global parameters, and A is the number of nucleon present in the nuclide (atomic mass). The keywords used for changing α, and β are alphald and betald, respectively. The gammashell1 and gammashell2 keywords are used to change γ_1, and γ_2, respectively.

Further, the spin cut-off parameter (σ^2) describes the angular distribution width of level density. It is possible to alter the spin cut-off parameter using the Rspincut keyword. This parameter can be defined as $\sigma^2 = \sigma_{\parallel}^2 = \mathrm{I_0t}$. where $\sigma_{\parallel}^2$ is the parallel component of the spin cut-off parameter, $\mathrm{I_0t}$ is the moment of inertia of the nuclide (undeformed) and t is the thermodynamic temperature. The perpendicular component $\sigma_{\perp}^2/\mathrm{t}$ is not constant from the point of view of the microscopic approach [17]. However, by considering the shell effects analogous to level density parameter (b), and then the adopted formula is,

$$\sigma^2 = I_0 \frac{b}{\tilde{b}} t \tag{3.4}$$

where, moment of inertia, $I_0 = \frac{\frac{2}{5} m_0 R^2 A}{(\hbar c)^2}$ and thermodynamic temperature t = $\sqrt{\frac{U}{b}}$. R is the radius of the nuclei (R = $\mathrm{R_0\ A^{1/3}}$), and $\mathrm{m_0}$ is the mass of the neutron in amu.

Using these expressions, the spincut parameter is defines as below,

$$\sigma^2 = 0.01389 \frac{A^{\frac{5}{3}}}{\tilde{b}} \sqrt{bU} \tag{3.5}$$

These parameters are altered to achieve fine fitting of the present and previously reported experimental data for ^{110}Cd(p, n) reaction.

3.2.3 Gamma transmission coefficient & Gamma ray strength functions (γ-SF)

Gamma transition in nuclear reactions can be described utilizing the γ-SF. The γ ray strength functions are also called radiative/photon strength functions. The γ-SF enter as a significant ingredient for the measurement of capture reaction cross section in the compound nucleus (CN) model, the evaluation of the gamma ray and particle emission, isomeric state calculations, and production of gamma ray spectra. The most admissible multi-polarities are electric dipole E_1, electric quadrupole E_2, and magnetic dipole M_1. Generally, Electric transitions are more dominant compare to magnetic transitions for a given multipolarity e.g. $f_{E_1}(E_\gamma) \gg f_{M_1}(E_\gamma)$

Various phenomenological and microscopic models for the γ-SF are implemented in TALYS.

strength 1: Kopecky-Uhl model [18]
This model uses generalized Lorentzian form. (default option)

strength 2: Brink-Axel Lorentzian [19]
It is the oldest model which describes giant dipole resonance (GDR) shape with the help of standard Lorentzian form. An option for all multi-poles higher than 1.

strength 3: Hartree-Fock BCS tables [20]
Goriely and Khan has calculated γ-SF and the models is stored as tables.

strength 4: Hartree-Fock-Bogolyubov tables [21]
This model has been stored as tables.

strength 5: Hybrid model [22]
Goriely has developed this Lorentzian model with temperature and energy dependent width that provides results in a different functional form at low energy than that of Kopecky-Uhl.

strength 6: Goriely T-dependent HFB
The temperature dependence is included in the Skyrme-HFB model with QRPA introduced by Goriely *et al.* [21].

strength 7: T-dependent RMF [23]
The model was developed by Goriel and Daoutidis.

strength 8: Gogny D1M HFB+QRPA [24]
Goriely has implemented the D1M version of the Gogny force and can be utilized for adjusting the tables.

A total of 96 different combinations of the basic constituent of the nuclear model, i.e., two default options of OMP, six default options of NLD models, and the eight default options of γ-SF were utilized for the theoretical cross section predictions of proton induced reaction such as ^{114}Cd(p, γ)^{115m}In, ^{114}Cd(p, n)^{114m}In, and ^{112}Cd(p, γ)^{113m}In reactions. The combination of these models has been explained in Chapter 6.

3.3 EMPIRE code

This code consists of different nuclear reaction modules that communicate with other modules included in the form of subroutines so it is called a modular system. It is widely utilized for the investigation of nuclear reactions and nuclear data estimation for large energy ranges. The code accepts nucleons (neutrons, protons), photons, alpha, helions, triton, deuteron, or other heavy ions as projectiles. The acceptable

energy range for this code is from just above the resonance range of neutrons ($\sim$ keV) to the hundredth of MeV for heavy ion-induced reactions. The input parameters requires for the calculation such as fission barriers, optical model parameters, deformation parameters, information of discrete level, nuclear masses, NLDs, and γ-SF were utilized from the RIPL-3 library. The output obtained from this code is converted to ENDF-6 format using EMPEND code.

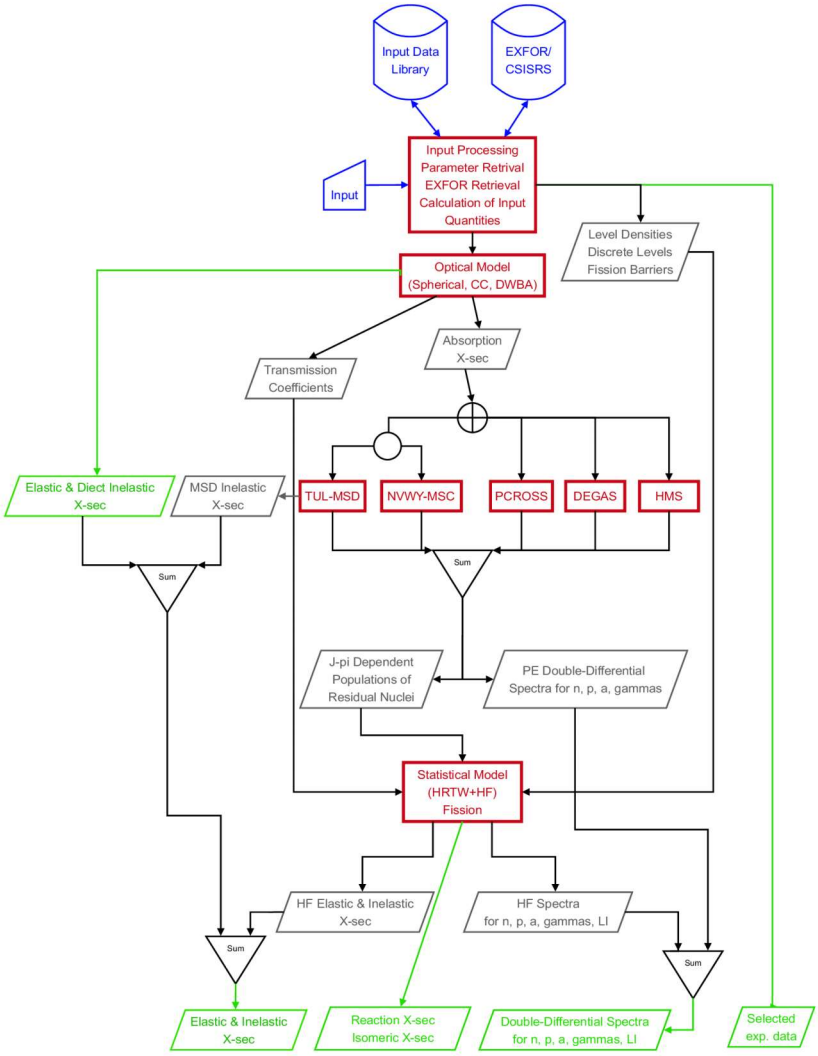

Figure 3.3: A Flow-chart explains the core physics of EMPIRE [34].

Various nuclear reaction models included in the code are mentioned here. A

generalized optical model (OM) - ECIS or coupled-channel calculations are used to study the direct reactions. The DWBA and Coupled-Channel codes, developed by J. Ranyal *et al.* [25,26] have been included in ECIS. The EMPIRE has five preequilibrium (PE) modules for studying the emission of nucleons, γ, and clusters from the complex nuclei just before it acquires the thermal equilibrium. The important energy range for the PE mechanism is the incident energy of the nucleons around 10 MeV and more. Three classical approaches of PE studies are the exciton model with angular momentum conservation-DEGAS code was developed by E. Bětak and P. Oblǒzinsky, and the PCROSS exciton model [27] based on the master equation solution [28]; and suggested by Cline [29] and Ribansky [30], and the Monte-Carlo simulation with linear momentum conservation (DDHMS) by M.B. Chadwick, and two quantum-mechanical approaches are deformation dependent multi-step direct (MSD) proposed by Tamura, Udagawa and Lenske [31] and Multi Step Compound (MSC) approach given by Nishioka *et al.* [32]. Additionally, EMPIRE code is coupled with KALMAN code which is used for the parameter fitting and covariance generation. The original coding of Kawano [33] has been used for KALMAN and it was assessed by Rochman and Pigni.

3.3.1 Level Densities (LDs)

EMPIRE consists of three phenomenological NLDs and one microscopic NLDs that describes several parameterizations of level densities. A parity distribution is expressed as ρ(E, J, π) = $\frac{1}{2}$ ρ(E, J) for each case, only the microscopic model is an exception as it uses tabulated RIPL-3 level densities (parity dependent). All the models are normalized to regenerate the neutron resonanceâĂŹs average parameters and the data on the progressive low-lying nuclear levels. The well-known and used level density model is the FGM.

☞ **LEVDEN 0**: EMPIRE-Specific Level Density (ESLD)

- The effective approach to the LDs is specific and it takes collective enhancements due to nuclear rotation and vibrations into consideration.

- The superfluid model is applied below a critical excitation energy, and the FGM is applied above it.

☞ **LEVDEN 1**: Generalized Superfluid Model (GSM) [12,13]

- The model is based on a phase transition from the superfluid at the lower energy wherever the level density is affected by pairing correlation to higher energy where FGM is applied.
- The model is similar to the GC model for the energy where low and higher energy can be distinguished from each other.

☞ **LEVDEN 2**: Gilbert-Cameron level densities (GCM) [10]

- The excitation energy splits into two regions. The CTM formula is applied at low excitation energy which is below the matching point (U) and the formula of FGM is applied above.

$$\rho^{GC}(E_x) = \begin{cases} \rho^{CT}(E_x) E_x \leq U \\ \rho^{FG}(E_x) E_x > U \end{cases} \tag{3.6}$$

- The constant or energy dependent LD parameter can be used for the calculations. The constant parameter (a) is read from GCROA input and energy dependent parameter considers the shell effects which will fade out as energy increases.
- Three relevant systematics of Iljinov *et al.* [35], Arthur [36], and Ignatyuk *et al.* [37] are available in EMPIRE.

☞ **LEVDEN 3**: Microscopic HFBCS level density

- The pre-calculated LDs using the Hartree-Fock-BCS approach for more than 8000 nuclei are tabulated in the RIPL library and can be used by EMPIRE.
- The approach is based on a single particle LD scheme for thermodynamic quantities determination.
- The HFB method with Skyrme force was used to create the particle-hole state densities as a function of E_x.

- These single particle levels have carried out the calculations in the prediction of nuclear masses and other properties of the ground state that convinced the level density calculation using this approach.
- The results includes constant treatment of deformation effects, shell corrections, rotational enhancement, and pairing correlations.

In our research work, the NLD models were used for the cross section predictions, all other default models are taken into account.

3.4 ALICE code

The ALICE-2014 is a Monte Carlo-based nuclear reaction code. The code consists of various nuclear theories for nuclear data evaluation. The code employs mainly Monte-Carlo formulations to study the decay of pre-compound nuclei [38], Weisskopf-Ewing evaporation [39] to study the equilibrium emission part, Bohr Wheeler fission [40], and for the light nuclei a Fermi statics break up model. The linear conservation model of Chadwik-Oblozinsky calculates the angular distribution [41].

The code accepts photons, neutrons, protons, and heavy ions, e.g. ^{4}He and heavier as incident particles. Targets from Beryllium up are possible, though light elements can present problems for trust in results. The excitation energy range is from 0.1 MeV to 1 GeV for projectile-target systems, the uncertainty in data prediction is observed for the energies above 200 MeV due to the lack of pion channel implication.

3.4.1 Nuclear level density models

ALICE includes four NLD options which are mentioned below.

Fermi Gas, Back-shifted pairing energies (FG) (default option)

Kataria-Ramamurthy and Kapoor (KR) [42]

Obninsk (OB) [43]

Gilbert-Cameron

The NLD model and the PLD parameter are changeable to obtain the most significant fit of experimental data. The Obnisk and Kataria-Ramamurthy do not have any adjustable parameters. The PLD can be calculated as, $a_{PLD} = A/9$, where, A is the number of nucleons of the composite nucleus. Presently, we have performed calculations with the default NLD options.

3.5 MCNP code

The Monte Carlo N-particle Transport (MCNP) code is a Monte Carlo-based geometry-dependent, time-dependent, general-purpose, N-particle transport computer code, developed and managed by Los Alamos National Laboratory. This code has been designed for studying the transport of gamma rays, neutrons, protons, and other particles as well as can transport secondary γ rays that emerge from the neutrons interaction. Also, the electrons, primary and secondary electrons that emerge from the γ interaction can be tracked by this code. MCNP is a versatile code used worldwide for various applications such as reactor design, ADSs research, designing of spallation targets, charged-particle and neutron transport for low energy applications, dosimetry, shielding design, medical physics and many more [44–46].

Without modifying the code, it is possible to calculate different radiation quantities. For the calculation, it is necessary to create an input file which defines the problem such as the specification of geometry and source, material description, location and specification of source, type of desired output and variance reduction techniques to use the code more effectively. The input file mainly contains three blocks, (i) Cell card, (ii) Surface card, and (iii) Data card. Geometry problems can be specified using Cell and Surface cards. The details of each card can be found in the MCNP user manual (vol. I) [47] as well as in the MCNP primer [45].
(i) Cell card: The cell card basically defines the volume shape by Boolean operation of the surfaces defined using the surface card. In this card, the first entry should be the cell number and it must begin within the first five columns. Three-dimensional

geometry using a Cartesian Coordinate system is defined by a cell card. The cells are bounded by surfaces that can be defined using Boolean expressions such as intersections, unions, and complements of regions. The basic cell card format is presented below for better understanding.

I M D GEOM PARAMS

I = the cell number (begin in first five column)
M = material number (If cell is void then M = 0),
D = cell material density,
= positive entry interprets the atomic density in order of 10^{24} atoms/cm^3
= negative entry interprets mass density (g/cm^3)
= no density entered reads void cell
GEOM = list of the signed bounding surfaces
PARAMS = optional cell parameters.

(ii) Surface card: It specifies the parameters of surfaces that bound a cell. One can define a sphere, plane, cylinder or any 2D shape acceptable with certain parameters defined in the MCNP user manual [46]. MCNP has used defined surfaces in the form of mnemonics to create the geometry of the problem. A surface is expressed as f(x, y, z) = 0. The basic surface card format is presented below.

I A LIST

I = unique surface number,
A = alphabetic mnemonic defines type of surface,
LIST = surface parameters.

(iii) Data card: The main and important card of MCNP input is the Data card which describes the whole simulation model except geometry specification. This card defines radiation source, type of particles, materials problem, cross section libraries, how to tally results, variance reduction technique, and many more.

The SDEF (Source DEFination) card defines the basic characteristic of the source. The card defines the position, particle type, energy, and dimension of the source. This single command can produce an incredible variety of sources. The material specification card can define the isotopic composition of the material, unique material number and evaluation of the cross section to be used in cells. The tally cards specify

the information one wants to extract from the Monte Carlo simulation. One or More tally cards can be used to extract the information. Many of the tally cards describe tally "bins" such as energy, time, and cosine bin cards. Seven standard tally cards are provided by MCNP. Tallies can be identified by type of the particle and tally. The numbers 1 to 8 or increment of 10 and particle designator: N for neutron, : for pion etc. are given to tallies. A list of tallies is presented in Table 3.1.

Table 3.1: Types of tallies given in MCNP.

Mneumonic	Tally type
F1	surface current
F2	average surface flux
F4	average flux in a cell
FMESH4	track-length tally over 3D mesh
F5a	flux at a point or ring
FIP5	pin-hole flux image
FIR5	planar radiograph flux image
FIC5	cylindrical radiograph flux image
F6	energy deposition
F7	fission energy deposition in a cell
F8	pulse height distribution in a cell

The information about the Mnemonic of geometry specification, cell, surface, and data cards are provided in ref. [45, 46].

To carry out the present work, the above codes were used to predict different important parameters. For example, the cross section values for different energies have been calculated using TALYS, EMPIRE, and ALICE codes, whereas the MCNP code was utilized to calculate the particle profile in the sample.

Bibliography

[1] A. Koning, S. Hilaire, S. Goriely, TALYS-1.9 - A Nuclear Reaction Program, User Manual, 1st edn (NRG, Westerduinweg, 2017).

[2] R. Capote *et al.*, Nucl. Data Sheets **110**, 3107-3214 (2009).

[3] J. Raynal, Notes on ECIS94, CEA Saclay Report No. CEA-N-2772, (1994).

[4] A. J. Koning and J. P. Declaroche, Nucl. Phys. A **713**, 231 (2003).

[5] E. Bauge, J. P. Delaroche, and M. Girod, Phys. Rev. C **63**, 024607 (2001).

[6] Kalbach, Phys. Rev. C **33**, 818 (1986).

[7] W. Hauser and H. Feshbach, Phys. Rev. **87**, 366 (1952).

[8] P. E. Hodgson, Rep. Prog. Phys. **34**, 765-819 (1971).

[9] J. P. Delaroche, Ch. Lagrange, and J. Salvy, IAEA-190, Vol. **1**, (Vienna, 1976), p. 25.

[10] A. Gilbert and A. G. W. Cameron, Can. J. Phys. **43**, 1446 (1965).

[11] W. Dilg *et al.*, Nucl. Phys. A **217**, 269 (1973).

[12] A. V. Ignatyuk, K. K. Istekov, and G. N. Smirenkin, Sov. J. Nucl. Phys. **29** (4), 450 (1979).

[13] A. V. Ignatyuk *et al.*, Phys. Rev. C **47**, 1504 (1993).

[14] S. Goriely *et. al.*, At. Data Nucl. Data Tables **77**, 311-381 (2001).

[15] S. Goriely, S. Hilaire, and A. J. Koning, Phys. Rev. C **78**, 064307 (2008).

[16] S. Hilaire and S. Goriely, Nucl. Phys. A **779**, 63âĂŞ81 (2006).

[17] S. Goriely, Nucl. Phys. A **605**, 28 (1996).

[18] J. Kopecky and M. Uhl, Phys. Rev. C **41**, 1941 (1990).

[19] D. M. Brink, Nucl. Phys. **4**, 215 (1957); P. Axel, Phys. Rev. **126**, 671 (1962).

[20] S. Goriely and E. Khan, Nucl. Phys. A **706**, 217 (2002).

[21] S. Goriely, E. Khan, and M. Samyn, Nucl. Phys. A **739**, 331 (2004).

[22] S. Goriely, Phys. Lett. B **436**, 10 (1998).

[23] I. Daoutidis and S. Goriely, Phys. Rev. C **86**, 034328 (2012).

[24] S. Goriely *et al.*, Phys. Rev. C **98**, 014327 (2018).

[25] J. Raynal, Technical Report No. SMR-9/8, IAEA (unpublished).

[26] J. Raynal, Computing as a language of physics. ICTP International Seminar Course (IAEA, ICTP, Trieste, Italy, 1972), p. 281.

[27] J. J. Griffin, Phys. Rev. Lett. **17**, 478 (1966).

[28] C. K. Cline and M. Blann, Nucl. Phys. A **172**, pp. 225-259 (1971).

[29] C. K. Cline, Nucl. Phys. A **193**, pp. 417-437 (1972).

[30] I. Ribanský, P. Oblǒzinský, and E. Bětak, Nucl. Phys., vol. A **205**, pp. 545-560 (1973).

[31] T. Tamura, T. Udagawa, and H. Lenske, Phys. Rev. C **26**, 379 (1982).

[32] H. Nishioka, J. J. M. Verbaarschot, H. A. Weidenmüller, and S. Yoshida, Ann. Phys. **172**, 67 (1986).

[33] T. Kawano and K. Shibata, Japan Atomic Energy Research Institute, Tokai, Japan, (1997).

[34] M. Herman *et al.*, Nucl. Data Sheets **108**, 2655-2715 (2007).

[35] A. Iljinov *et al.*, Nucl. Phys. A **543**, 517 (1992).

[36] P. G. Young *et al.*, Trans. Amer. Nucl. Soc. **60**, 271 (1989).

[37] A. V. Ignatyuk, G. N. Smirenkin, and A. S. Tishin, Sov. J. Nucl. Phys. **21**, 255 (1975).

[38] M. Blann, Phys. Rev. C **54**, 1341 (1996).

[39] V. F. Weisskopf and D.E. Ewing, Phys. Rev. **57**, 472 (1940).

[40] N. Bohr and J. A. Wheeler, Phys. Rev **56**, 426 (1939).

[41] M. B. Chadwick and P. Oblozinsky, Phys. Rev. C **50**, 2490 (1994).

[42] S. K. Kataria, V. S. Ramamurthy, and S. S. Kapoor, Phys. Rev. C **18**, 549 (1978).

[43] A. V. Ignatyuk *et al.*, Phys. Rev. C **47**, 1504 (1993).

[44] T. Goorley *et. al.*, "Features of MCNP6", Supercomputing in Nuclear Applications and Monte Carlo 2013, Paris, Oct 27-31, LA-UR-13-28114 (2013).

[45] J. K. Shultis and R. E. Faw, An MCNP Primer (2011).

[46] MCNP Users Manual **-** Code Version 6.2, edited by C. J. Werner, Los Alamos National Laboratory Report No. **LA-UR-17-29981**, 2017 (unpublished).

[47] J. E. Sweezy *et al.*, Los Alamos National Laboratory Tech. Rep. **LA-UR-03-1987 (Revised 2/1/2008).** Los Alamos, NM, USA. (2003).